NO_3^--induced pH Changes in Mammalian Cells
Evidence for an NO_3^--H^+ Cotransporter

Chung-Wai Chow,*‡ Andras Kapus,‡ Robert Romanek,‡ and Sergio Grinstein‡

From the *Division of Respiratory Medicine, Department of Medicine, University of Toronto; and ‡Division of Cell Biology, Research Institute, The Hospital for Sick Children, Toronto M5G 1X8, Canada

ABSTRACT The effect of NO_3^- on intracellular pH (pH_i) was assessed microfluorimetrically in mammalian cells in culture. In cells of human, hamster, and murine origin addition of extracellular NO_3^- induced an intracellular acidification. This acidification was eliminated when the cytosolic pH was clamped using ionophores or by perfusing the cytosol with highly buffered solutions using patch-pipettes, ruling out spectroscopic artifacts. The NO_3^--induced pH change was not due to modulation of Na^+/H^+ exchange, since it was also observed in Na^+/H^+ antiport-deficient mutants. Though NO_3^- is known to inhibit vacuolar-type (V) H^+-ATPases, this effect was not responsible for the acidification since it persisted in the presence of the potent V-ATPase inhibitor bafilomycin A_1. NO_3^-/HCO_3^- exchange as the underlying mechanism was ruled out because acidification occurred despite nominal removal of HCO_3^-, despite inhibition of the anion exchanger with disulfonic stilbenes and in HEK 293 cells, which seemingly lack anion exchangers (Lee, B.S., R.B. Gunn, and R.R. Kopito. 1991. *J. Biol. Chem.* 266:11448–11454). Accumulation of intracellular NO_3^-, measured by the Greiss method after reduction to NO_2^-, indicated that the anion is translocated into the cells along with the movement of acid equivalents. The simplest model to explain these observations is the cotransport of NO_3^- with H^+ (or the equivalent counter-transport of NO_3^- for OH^-). The transporter appears to be bi-directional, operating in the forward as well as reverse directions. A rough estimate of the fluxes of NO_3^- and acid equivalents suggests a one-to-one stoichiometry. Accordingly, the rate of transport was unaffected by sizable changes in transmembrane potential. The cytosolic acidification was a saturable function of the extracellular concentration of NO_3^- and was accentuated by acidification of the extracellular space. The putative NO_3^--H^+ cotransport was inhibited markedly by ethacrynic acid and by α-cyano-4-hydroxycinnamate, but only marginally by 4,4′-diisothiocyanostilbene-2,2′ disulfonate or by *p*-chloromercuribenzene sulfonate. The transporter responsible for NO_3^--induced pH changes in mammalian cells may be related, though not identical, to the NO_3^--H^+ cotransporter described in *Arabidopsis* and *Aspergillus*. The mammalian cotransporter may be important in eliminating the products of NO metabolism, particularly in cells that generate vast amounts of this messenger. By cotransporting NO_3^- with H^+ the cells would additionally eliminate acid equivalents from activated cells that are metabolizing actively, without added energetic investment and with minimal disruption of the transmembrane potential, inasmuch as the cotransporter is likely electroneutral.

KEY WORDS: nitrate • proton • ion transport • pH regulation

INTRODUCTION

Nitric oxide has been recently recognized as an important second messenger in a variety of cell types. The generation of NO from L-arginine is catalyzed by NO-synthase in response to a number of stimuli including bacterial lipopolysaccharide, tumor necrosis factor-α, and γ-interferon (see Kiechle and Malinski, 1993; Anggard, 1994; Weinberg et al., 1995 for review). NO is an unstable intermediate compound which, in aerobic aqueous solutions such as the cytosol, is rapidly metabolized primarily to nitrite (NO_2^-) and to a lesser extent to nitrate (NO_3^-). In the presence of oxidizing species such as oxyhemoproteins, NO_2^- is rapidly converted to the more stable NO_3^- (Ignarro et al., 1993; Veszelovszky et al., 1995). Lipopolysaccharide and cytokine-induced formation of NO, NO_2^-, and NO_3^- in vitro has been extensively reported in neutrophils, primary macrophages, and monocyte/macrophage cell lines (Iyengar et al., 1987; Miwa et al., 1987; Schmidt et al., 1989; Wright et al., 1989). In animal models, increased production of NO_3^- has been reported in sepsis (Ohshima et al., 1994; Oudenhoven et al., 1994; Wright et al., 1992), glomerulonephritis (Sever et al., 1992), and graft rejection (Tanaka et al., 1995; Winlaw et al., 1994; Drobyski et al., 1994). In humans, acute graft vs. host disease, bacterial and viral meningitis, acute gastroenteritis, and sepsis have been associated with increased NO_3^- production (Jungersten et al., 1993; Shi et al., 1993; Milstien et al., 1994; Weiss et al., 1995).

Address correspondence to Dr. Sergio Grinstein, Division of Cell Biology, Research Institute, The Hospital for Sick Children, 555 University Avenue, Toronto, ON M5G 1X8, Canada. Fax: 416-813-5028; E-mail: sga@resunix.ri.sickkids.on.ca

The amounts of NO_2^- and NO_3^- generated from NO are substantial. The cytosolic concentrations of NO_2^- and NO_3^- in stimulated macrophages were found to be 119.3 nmol/ml and 281.2 nmol/ml, respectively (Marletta et al., 1988). These figures greatly underestimate the amount produced, since NO_2^- and NO_3^- are not retained within the cell and can be readily recovered in the extracellular milieu. In in vitro experiments, 100–200 nmol of NO_2^- and NO_3^- were recovered from the medium bathing 10^6 stimulated macrophages (Stuehr and Marletta, 1987*a*, *b*, *c*; Miwa et al., 1991). Plasma nitrate levels as high as 200 μM have been reported in disease states such as acute gastroenteritis (Jungersten et al., 1993). These findings imply that NO_2^- and NO_3^- must be transported effectively across the plasma membrane for subsequent disposal. However, the pathway(s) for transport of NO_2^- and NO_3^- in mammalian cells are poorly understood.

This report describes a NO_3^- transport system present in a variety of mammalian cells. In the course of measurements of the anion dependence of the intracellular pH of Chinese hamster ovary (CHO)[1] cells, we made the serendipitous observations that addition of extracellular NO_3^- induced a reproducible cytosolic acidification. The purpose of this study was to characterize this NO_3^--induced cytosolic acidification, to compare the underlying mechanism with known pH_i regulatory systems, and to describe its pharmacological profile.

METHODS

Materials and Media

Nigericin, 2′7′ bis-(2-carboxyethyl)-5(and 6) carboxyfluorescein (BCECF) free acid and acetoxymethyl ester were purchased from Molecular Probes, Inc. (Eugene, OR). Antimycin A, 2-deoxy-D-glucose, 2-(*N*-morpholino)ethanesulfonic acid (MES), β-nicotinamide adenine dinucleotide phosphate (NADPH), glucose-6-phosphate, bafilomycin, 4,4′-diisothiocyanostilbene-2,2′ disulfonate (DIDS), α-cyano-4-hydroxycinnamate (CHC), and *p*-chloromercuribenzene sulfonate (pCMBS) were obtained from Sigma Chemical Co. (St. Louis, MO). Ethacrynic acid was purchased from Serva (Heidelberg, Austria) and phloretin from K+K (Hollywood, CA). Glucose-6-phosphate dehydrogenase and nitrate reductase were from Boehringer Mannheim (Indianapolis, IN). All other chemicals and salts were purchased from Sigma Chemical Co.

PBS contained (in mM): 140 NaCl, 10 KCl, 8 sodium phosphate, 2 potassium phosphate, pH 7.4. The sodium chloride solution contained (in mM): 117 NaCl, 1.66 $MgSO_4$, 1.36 $CaCl_2$, 5.36 KCl, 25 HEPES, 5.55 glucose. Sodium nitrate solution contained (in mM): 117 $NaNO_3$, 6.2 $MgSO_4$, 1.36 calcium gluconate, 5.36 potassium gluconate, 25 HEPES, 5.55 glucose. Sodium gluconate solution contained (in mM): 117 sodium gluconate, 6.2 $MgSO_4$, 1.36 calcium gluconate, 5.36 potassium gluconate, 25 HEPES, 5.55 glucose. Potassium and *N*-methyl-D-glucammonium (NMG) solutions were made with equimolar substitution of the appropriate salts. To study the nitrate concentration dependence we used media with $NaNO_3$ concentrations varying from 3.65 to 117 mM that were osmotically balanced with sodium gluconate. Sodium nitrite solutions containing 10–117 mM $NaNO_2$ were prepared similarly. Unless otherwise indicated, all solutions were titrated to pH 7.5.

The composition of the low-buffer solution used to fill the patch pipettes was (in mM): 1 MES, 120 KCl, 1 $MgCl_2$, 12 potassium gluconate, 50 glucose, 1 Mg-ATP, pH to 7.5 with NMG-OH. The high-buffer pipette solution contained (in mM): 50 HEPES, 50 Tris, 20 KCl, 1 $MgCl_2$, 12 potassium gluconate, 50 glucose, 1 Mg-ATP, pH to 7.3 with HCl. All pipette solutions also contained 300 μM BCECF-free acid. External solutions used in patch clamp experiments were composed of (in mM): 120 KCl, 1 $MgCl_2$, 12 KOH, 50 HEPES, pH 7.0. The potassium nitrate solution was made with equimolar substitution of KNO_3 for KCl. All solutions were nominally bicarbonate-free and were adjusted to 290 ± 10 mosM with the major salt.

Cells

WT5 is a sub-line of wild-type CHO cells. AP1 is a cell line derived from WT5 that is devoid of endogenous Na^+/H^+ activity (Rotin and Grinstein, 1989). HEK 293 is a human embryonic kidney cell line (Lee et al., 1991). J774 is a murine monocyte/macrophage cell line. Cells were grown in α-MEM (Ontario Cancer Institute, Toronto, ON) containing 25 mM $NaHCO_3$ supplemented with 10% FCS, 100 U/ml penicillin, and 100 μg/ml streptomycin (Life Technologies, Inc., Grand Island, NY) and were incubated in a humidified environment containing 95% air and 5% CO_2 at 37°C. Cultures were reestablished from frozen stocks regularly, and cells from passages 3 to 20 were used for the experiments.

Where indicated, intracellular ATP was depleted by incubating the cells for 10 min in glucose-free medium with 5 mM 2-deoxy-D-glucose and 1 μg/ml antimycin A, to inhibit both glycolysis and oxidative phosphorylation. This protocol has previously been shown to deplete >90% of the ATP in CHO cells within 10 min (Goss et al., 1994). Subsequent fluorescence measurements were performed in glucose-free media containing 5.5 mM 2-deoxy-D-glucose.

Measurements of Cytosolic pH

Microfluorimetry. The cytosolic pH (pH_i) of small groups of cells was determined by microphotometry of the fluorescence emission of BCECF using dual wavelength excitation. Cells grown to confluence on 25-mm glass coverslips (Thomas Scientific, Swedesboro, NJ) were loaded with BCECF by incubation with 2 μg/ml of the precursor acetoxymethyl ester form for 10 min at 37°C. The coverslips were then mounted in a Leiden Coverslip Dish (Medical System Corp., Greenvale, NY) and placed into a thermostatted holding chamber heated to 37°C (Open Perfusion Microincubator; Medical Systems Corp., Greenvale, NY) attached to the stage of a Nikon Diaphot TMD inverted microscope (Nikon Canada, Toronto, ON). Cells were visualized using a Nikon Fluor 40×/1.3 N.A. oil-immersion objective and a Hoffman modulation contrast video system with an angled condenser (Modulation Optics) through a CCD-72 video camera and control unit (Dage-MTI, Michigan City, IN) connected to a Panasonic monitor. Clusters of 6–12 cells from the confluent culture were selected for analysis with an adjustable diaphragm. The chamber

[1]Abbreviations used in this paper: AP1, CHO mutant; BCECF, 2′7′*bis*-(2-carboxyethyl)-5(and 6) carboxyfluorescein; CHC, α-cyano-4-hydroxycinnamate; CHO, Chinese hamster ovary; DIDS, 4,4′-diisothiocyanostilbene-2,2′ disulfonate; HEK, human embryonic kidney; NADPH, β-nicotinamide adenine dinucleotide phosphate; NHE, Na^+/H^+ exchangers; NMG, *N*-methyl-D-glucammonium; pCMBS, *p*-chloromercuribenzene sulfonate; V-ATPases, vacuolar-type H^+ pumps; (V) H^+-ATPases, vacuolar-type H^+-ATPases; WT5, wild-type CHO cell.

was continuously perfused at ≈0.5 ml/min to allow for complete exchange of the bath solution once every minute using a gravity-driven system and a Leiden aspirator. Solutions could be switched by opening solenoid valves (General Valve, Fairfield, NJ). When rapid solution changes were required, 3 aliquots of 1 ml of the new medium were quickly pipetted (<15 s) into the chamber and perfusion was continued using the new medium (Kapus et al., 1994).

Fluorescence measurements were made using an M Series Dual Wavelength Illumination System from Photon Technologies, Inc. (South Brunswick, NJ) in a dual excitation single emission configuration. Excitation light provided by a Xenon lamp was alternately selected using 495 ± 10 nm and 445 ± 10 nm filters (Omega Optical, Brattleboro, VT) at a rate of 50 Hz and then reflected to the cells by a 510-nm dichroic mirror. Emitted light was first selected by a 520 nm long-pass filter and then separated from the red light used for Hoffman imaging by a 550 nm dichroic mirror and directed to the photometer through a 530 ± 30 nm band-pass filter. This optical system allowed for continuous visualization of cells without interfering with fluorescence measurements. Photometric data was acquired at 10 Hz using a 12 bit A/D board (Labmaster, National Instruments, Austin, TX) interfaced to a Dell 486 computer and analyzed with the Felix software (Photon Technologies Inc.). Calibration of the fluorescence intensity to pH_i was performed in the presence of 5 μM nigericin in high potassium medium (140 mM KCl, 20 mM HEPES, 1 mM $MgCl_2$ and 5 mM glucose) as previously described (Thomas et al., 1979). Each coverslip was calibrated at the end of the experiment using at least three pH values.

Fluorescence Imaging. For imaging of single cell pH_i, cells were grown on round glass coverslips to 60–70% confluence and loaded with BCECF as described above. Ratio fluorescence imaging was performed on a Zeiss Axiovert 100 TV inverted microscope (Zeiss, Oberkochen, Germany) equipped with a 75 W Xenon lamp (XBO 75, Zeiss), a shutter/filter wheel assembly (Lambda 10, Sutter Instrument Co., Novato, CA), a NeoFluar 63×/1.25 N. A. objective and a high-resolution (1,317 × 1,025 pixels, KAF 1400, Kodak) cooled, digital CCD camera (TEA/CCD 1317; Princeton Instruments, Trenton, NJ) interfaced to a Pentium 90 computer (Dell Inc., Toronto, ON, Canada) via a 12 bit, 1 MHz camera-controller (Princeton controller: ST-38; Princeton Instruments, Trenton, NJ). Image acquisition and excitation filter selection were controlled by the Metafluor software (Universal Imaging Corp., West Chester, PA). All measurements of pH_i were performed at 37°C.

Electrophysiology and pH_i Measurements in Voltage-clamped Cells

Cells were patch-clamped in the whole-cell configuration of the patch clamp technique using an Axopatch-1D amplifier (Axon Instruments Inc., Foster City, CA), as described (Kapus et al., 1993). Electrodes were made from filament-filled borosilicate glass capillaries (World Precision Instruments Inc., Sarasota, FL) using a horizontal puller (P-87; Sutter Instrument Co., Novato, CA) and a microforge (MF-9; Narishige USA, Greenvale, NY). Pipette resistance ranged from 2 to 10 MΩ; seal resistance ranged from 10 to 50 GΩ. Series resistance varied between 5 and 30 MΩ, and cell capacitance was between 12 and 34 pF.

Cytosolic pH in voltage-clamped cells was measured microfluorimetrically on the Photon Technologies Inc. photometric system described above, using pipette solutions with a low buffering power (1 mM MES) to maximize the NO_3^--induced intracellular pH changes. Cells were patch-clamped in the whole-cell configuration and loaded with BCECF-free acid by diffusion of the dye from the pipette solution into the cytosol. Measurements were initiated 5 min after attaining the whole-cell configuration to allow for equilibration of the cytosolic pH with the pipette pH and for adequate BCECF loading. Cells were superfused at 0.5 ml/min with the indicated solutions. Calibration of fluorescence ratio vs. pH was performed on single nonpatched cells, using the nigericin technique described above (Thomas et al., 1979). One calibration curve was obtained every day by averaging data from 3 to 6 cells sequentially perfused with KCl media buffered at 3 different pH values ranging from 6.0 to 7.5. All patch clamp experiments were carried out at room temperature. Single-cell pH_i measurements were also performed microfluorimetrically in nonpatched cells at room temperature to ensure that the NO_3^--induced cytosolic acidification was present under these conditions as well (data not shown).

Measurements of Intracellular Nitrate Content

AP1 cells were grown to confluence on 6-well plastic tissue culture dishes (Costar Corp., Cambridge, MA). Culture medium was aspirated and cells were incubated with isotonic $NaNO_3$ solution at 0 or 37°C for the indicated times. Where indicated, the solution contained 100 μM DIDS. At the end of the incubation period, each well was rapidly washed 3 times with 10 ml of PBS at 4°C and subsequently the cells were lysed using 1 ml distilled water and repeated freeze-thawing. Whole cell lysates were centrifuged for 10 min in a microcentrifuge (Beckman Microfuge, 13,500 rpm; Beckman Instruments, Fullerton, CA) to remove cellular debris. The NO_3^- content of the resultant supernatant was measured using the Greiss reaction after reduction of NO_3^- to NO_2^-, as previously described (Green et al., 1982; Verdon et al., 1995; Gilliam et al., 1993). Reduction of NO_3^- to NO_2^- was performed by incubating the supernatant with 1 μM NADPH, 0.16 U/ml glucose-6-phosphate dehydrogenase, 500 μM glucose-6-phosphate, and 0.80 U/ml nitrate reductase at room temperature for 45 min. A 500-μl aliquot of the sample was then incubated with 250 μl of 0.1% (*N*-1-naphthyl)-naphthylethylene diamine dihydrochloride and 250 μl of 1% sulfanilamide in 5% phosphoric acid at 37°C for 10 min. Absorbance was measured spectrophotometrically at 540 nm in a Hitachi U-2000 spectrophotometer. A calibration curve was constructed by adding increasing concentrations of $NaNO_3$ to lysates of cells not exposed to exogenous NO_3^-. A second aliquot of the cell lysate was used for protein determination using the BioRad Protein Assay Kit (BioRad Laboratories, Richmond, CA). Total cell number was estimated by normalizing the protein content in the whole cell lysate to that of a cell suspension containing a known number of cells, determined electronically using the Coulter counter. The cell suspension was prepared by addition of 1 ml of trypsin-EDTA (GIBCO-BRL, Life Technologies Inc., Grand Island, NY) to AP1 cells grown to confluence in a 75-ml tissue culture flask. The volume of the suspended cells was determined with the Coulter-Channelyzer combination. The intracellular NO_3^- concentration was then calculated by dividing the NO_3^- content of the cell lysate by the corresponding cellular volume.

Data Analysis and Statistics

Quantification of cell-associated fluorescence was performed using the Felix software package (Photon Technologies, Inc.) or the Metamorph/Metafluor package (Universal Imaging, Inc., West Chester, PA). Mean $H^+_{(equivalent)}$ flux was calculated by multiplying the rate of pH_i change ($\Delta pH_i/\Delta time$) by the buffering capacity of CHO cells, measured to be 25 mmol/pH/liter of cells in the pH range of our measurements (Kapus et al., 1994). The rate of pH_i change was derived by linear regression of the pH_i vs. time curve over 4-s intervals using the Origin software (MicroCal Software Inc., Northampton, MA). Data were graphed using the Ori-

gin software and are shown as mean ± one standard error (SE) of the number of experiments indicated. Significance was calculated using Student's *t* test.

RESULTS

Effect of Nitrate on Intracellular pH

The effect of external NO_3^- on pH_i was evaluated microfluorimetrically in CHO cells loaded with BCECF. To facilitate the detection of NO_3^--induced changes in pH_i, the contribution of other acid/base transporters, which might have a compensatory effect, was minimized. For this purpose, the initial experiments were performed in nominally HCO_3^--free and Na^+-free solutions, to minimize Cl^-/HCO_3^- exchange and Na^+-dependent acid/base transport. As shown in Fig. 1 *A*, superfusion of the cells with an NO_3^--rich solution induced a sizable cytosolic acidification. The change in pH_i cannot be attributed to removal of external Cl^-, since substitution of Cl^- with equimolar gluconate$^-$ did not significantly alter pH_i. This finding also implies that Cl^-/HCO_3^- exchange activity is negligible, since the alkalinization predicted to result from uptake of HCO_3^-, in exchange for exiting Cl^-, was not detectable. It is therefore unlikely that the NO_3^--induced acidification results from exchange with intracellular HCO_3^- via the anion exchanger.

It was important to ascertain that the NO_3^--induced acidification of the cells is neither artifactual nor the result of a toxic effect. Cell morphology, which was monitored continuously using Hoffman optics, was not altered by addition of NO_3^-. Moreover, BCECF was retained by the cells throughout the observation period, attesting to the viability of the cells. Finally, the effect of external NO_3^- was reversible since reperfusion with the Cl^--rich medium induced recovery of pH_i (Fig. 1 *A*). These observations argue against a deleterious effect of NO_3^-.

In our experiments, pH_i is estimated from the ratio of BCECF fluorescence recorded at two excitation wavelengths. Differential quenching of fluorescence at one of these wavelengths by NO_3^- could mimic the appearance of acidification. Several experimental approaches were used to rule out this potential artifact. We first compared the spectral properties of the free acid of BCECF in vitro in isotonic KCl or KNO_3 solutions, titrated to pH levels ranging from 5.84 to 7.56 with HCl or HNO_3. Excitation and emission spectra acquired in Cl^- and NO_3^- solutions were identical (data not shown). That NO_3^- does not alter the behavior of the dye inside cells was shown by clamping pH_i with 5 μM nigericin, a K^+/H^+ ionophore, in cells bathed in media containing 140 mM K^+. Under these conditions the fluorescence ratio was unaffected by substitution of extracellular Cl^- for NO_3^- (Fig. 1 *B, right*).

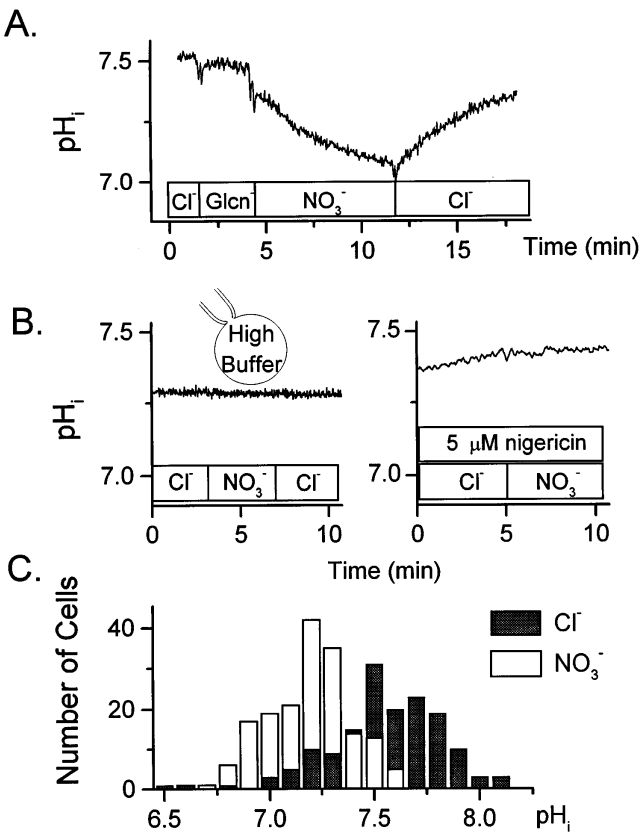

FIGURE 1. NO_3^--induced cytosolic acidification in Chinese hamster ovary (CHO) cells. (*A*) CHO (AP1) cells grown to near confluence on glass coverslips were loaded with BCECF and used for microfluorimetric determination of pH_i. The coverslip was perfused sequentially with the following K^+-rich solutions, as indicated by the bar at the bottom of the graph: Cl^-, gluconate$^-$, NO_3^-, and Cl^-. Trace is representative of 4 similar experiments. (*B, left*) A single CHO cell was patched in the whole-cell configuration with a pipette filled with high buffer solution (50 mM HEPES, 50 mM Tris, 20 mM KCl) containing BCECF and used for microfluorimetric determination of pH_i. After equilibration of the cytosol with the pipette buffer (~5 min), the extracellular bathing medium was changed from KCl solution to KNO_3 solution, as indicated. The trace is representative of 2 experiments. (*right*) CHO cells grown to near confluence on glass coverslips were loaded with BCECF and used for microfluorimetric determination of pH_i. The pH_i of the cells was clamped by incubation with 5 μM nigericin in a K^+-rich solution for 5 min. Where indicated, the main anion of the perfusing solution was switched from Cl^- to NO_3^-, while keeping the K^+ concentration constant at 140 mM. The trace is representative of 5 similar experiments. (*C*) CHO cells were grown to 60–70% confluence on coverslips and loaded with BCECF for measurement of pH_i by ratio imaging. The cells were allowed to equilibrate with the isotonic Cl^--rich solution and one set of images was acquired (*solid bars*). The solution was then substituted for a NO_3^--rich medium, and, after 5 additional min, another set of images was acquired (*open bars*). Images were collected from multiple areas of the coverslip while continuously perfusing the coverslip with the indicated solution. Quantification of cell-associated fluorescence ratio was performed using the Metamorph/Metafluor package (Universal Imaging, Inc.). Calibration of fluorescence ratio vs. pH_i was performed on the same coverslip using the nigericin technique, as described in EXPERIMENTAL PROCEDURES. The histogram was built using 153 and 174 cells perfused with isotonic Cl^--rich and NO_3^--rich media, respectively.

The effects of extracellular NO_3^- on pH_i were also eliminated when the buffering capacity of the cytosol was greatly increased. This was accomplished by patch-clamping CHO cells in the whole-cell configuration with pipettes filled with a high buffer (50 mM HEPES, 50 mM Tris) solution. Microfluorimetric measurements of the individual patched cells revealed no change in pH_i when extracellular Cl^- was replaced by NO_3^- and vice versa (Fig. 1 *B*, *left*). Together, these findings indicate that NO_3^- does not artifactually alter the fluorescence of BCECF and indicate that this anion induces a bona fide change in pH_i.

Microfluorimetric measurements like those of Fig. 1 *A* represent the average pH_i of clusters of 6–12 cells. To assess whether the NO_3^--induced cytosolic acidification occurs in all or most of the cells in the population and to further validate the microfluorimetric observations, the pH_i of individual cells was measured by ratio fluorescence imaging, as described in EXPERIMENTAL PROCEDURES. For these experiments, CHO cells were grown to submaximal confluence on glass coverslips, to facilitate the demarcation of individual cells, and were loaded with BCECF as described. Cells were perfused for 5 min in isotonic Cl^- or NO_3^- solution before image acquisition, to allow adequate time for equilibration. As shown in Fig. 1 *C*, NO_3^--induced cytosolic acidification occurred in virtually all the cells studied (n = 153 cells in Cl^--rich solution and n = 174 in NO_3^--rich solution). The mean pH_i in Cl^- solution was 7.55 ± 0.02, whereas 5 min after switching to NO_3^-, pH_i had decreased to 7.19 ± 0.02. These values were statistically different with $P = 2.84 \times 10^{-34}$ (Student's t test). It is noteworthy that the recording systems used for the imaging and photometry experiments are entirely different, indicating that the pH changes recorded are independent of the optical path, detector, and analysis software used.

We also tested whether other cell types also display the NO_3^--induced changes in pH_i. The murine monocyte-macrophage cell line J774 was tested since, as detailed in the INTRODUCTION, NO_3^- production is greatly enhanced in stimulated phagocytes (Miwa et al., 1987; Iyengar et al., 1987; Schmidt et al., 1989; Wright et al., 1989). When bathed in NO_3^--rich media, J774 cells underwent a cytosolic acidification at a rate similar to that observed in CHO cells (Table I).

TABLE I

NO_3^--induced Acidification in Different Cell Types

Cell type	n	$H^+_{(equivalent)}$ flux (mmol/liter cells/min)
CHO − WT5 (K^+-medium)	4	2.42 ± 0.80
CHO − WT5 (NMG^+-medium)	6	2.39 ± 0.39
CHO-AP1	4	2.03 ± 0.42
J774	3	1.71 ± 0.48
HEK	3	3.56 ± 0.68

pH_i was measured fluorimetrically in adherent, BCECF-loaded cells as described under METHODS. Cells were initially incubated with NMG-Cl solution and cytosolic acidification was induced by perfusion with NMG-NO_3 solution. Where specified, WT5 cells were perfused sequentially with KCl and KNO_3 solutions. $H^+_{(equivalent)}$ flux was derived by multiplying the rate of pH_i change (estimated over the first 60 s) by the buffering capacity of the cells, which was determined independently in the appropriate pH_i range (see METHODS). All experiments were performed at 37°C. Results shown are means ± one standard error of the number of experiments indicated (n).

NO_3^--induced Cytosolic Acidification Is Accompanied by NO_3^- Uptake

NO_3^- could induce the observed pH_i changes by acting on an extracellular receptor, by altering the transmembrane potential or by driving the transport or generation of acid equivalents as it enters the cell. To test whether the NO_3^--induced intracellular acidification is accompanied by entry of the anion into the cells, the intracellular NO_3^- content was measured using the Greiss method, after reduction of NO_3^- to NO_2^- (see EXPERIMENTAL PROCEDURES). For these experiments, CHO cells were incubated with isotonic $NaNO_3$ for 2–10 min at 37°C. Extracellular trapping was estimated by exposing cells momentarily to ice-cold $NaNO_3$ solution at 0°C (time = 0 in Fig. 2). Subtraction of this value from the individual determinations also accounted for any endogenous NO_3^- or NO_2^-. Uptake of NO_3^- by the cells was linear for at least 10 min. In cells incubated with 117 mM NO_3^- the initial rate of entry of the anion, derived from linear regression, averaged 6.75 ± 0.15 mmol/liter cells/min (n = 3 at 2 min; n = 6 for all other time points; R = 0.995).

Exchange of NO_3^- for Cl^- (Simchowitz, 1988; Simchowitz and Davis, 1989; Zhang and Solomon, 1992; Kurtz et al., 1994) has been documented to occur via the stilbene-sensitive anion exchanger (AE). To determine whether this process contributes to NO_3^- uptake in CHO cells, measurements were also performed in the presence of 100 μM 4,4′-diisothiocyanostilbene-2,2′-disulfonate (DIDS), a concentration of the inhibitor that is expected to completely block the AE1 (Bruce et al., 1994*a*, *b*) and AE3 (Lee et al., 1991) isoforms and largely block the AE2 isoform of the exchanger (Simchowitz and Davis, 1989; Lee et al., 1991). NO_3^- flux in DIDS-treated cells was 2.66 ± 0.07 mmol/liter cells/min (n = 3 at 2 min; n = 6 for all other time points; R = 0.994). Thus 39% of the total NO_3^- flux was insensitive to stilbenes and may be, at least in part, coupled to the translocation of H^+ equivalents (see below).

Since the NO_3^--induced pH_i changes were reversible, we tested the reversibility of the NO_3^- fluxes. In three experiments, NO_3^- content was measured in cells incubated with the anion for 15 min, followed by incubation in a NO_3^--free (Cl^--rich) medium for 10 min at

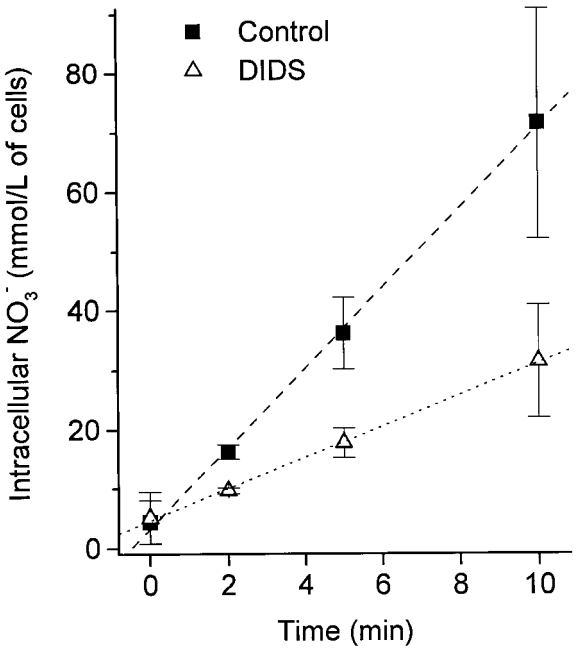

FIGURE 2. Time course of NO_3^- uptake by adherent CHO cells. CHO cells were grown to near confluence on 6-well plastic tissue culture dishes. The cells were exposed to $NaNO_3$ solution for the times indicated, then washed extensively in the cold. Following lysis using 1 ml distilled H_2O and repeated freeze-thawing, the intracellular NO_3^- content was measured after reduction to NO_2^- as described in EXPERIMENTAL PROCEDURES. *Solid squares*: control cells. *Open triangles*: the uptake medium contained 100 μM 4,4′-diisothiocyanostilbene-2,2′ disulfonate (DIDS). Cell number and cell volume were measured using the Coulter-Channelyzer in parallel samples of cells that were suspended by trypsinization. Data are means ± SE of 3 determinations at 2 min and 6 experiments at other time points. Lines were fitted by linear regression.

37°C. Upwards of 85% of the NO_3^- taken up by the cells was lost during the washout period, implying that transport of the anion is bi-directional (data not shown).

Jointly, these experiments indicate that NO_3^- is transported across the membrane during the course of the NO_3^--induced pH_i changes. The flux of NO_3^- may alter pH_i directly, by driving the transport of H^+ equivalents across the membrane through a formerly unidentified pathway. Alternatively, the anion could conceivably modulate the activity of known acid/base transporters, such as Na^+/H^+ exchangers (NHE), anion exchangers or vacuolar-type H^+ pumps (V-ATPases). These possibilities were considered experimentally below.

NO_3^--induced Cytosolic Acidification Is Not Mediated by the Na^+/H^+ Antiporter

In erythrocytes, NHE has been reported to be inhibited by NO_3^- (Parker, 1983; Parker and Castranova, 1984; Jennings et al., 1986). Because NHE is thought to contribute to the maintenance of the steady-state pH_i, inhibition of this transporter by NO_3^- could conceivably result in a cytosolic acidification like that illustrated in Fig. 1 *A*. To test this hypothesis, we compared the effect of NO_3^- on pH_i changes in two clones of CHO cells, the wild-type CHO cell (WT5) which expresses the NHE-1 isoform of the exchanger and the CHO mutant (AP1) which is devoid of NHE. As illustrated in Fig. 3 *A*, WT5 cells recover readily from an acid load upon addition of extracellular Na^+. Such recovery, which is inhib-

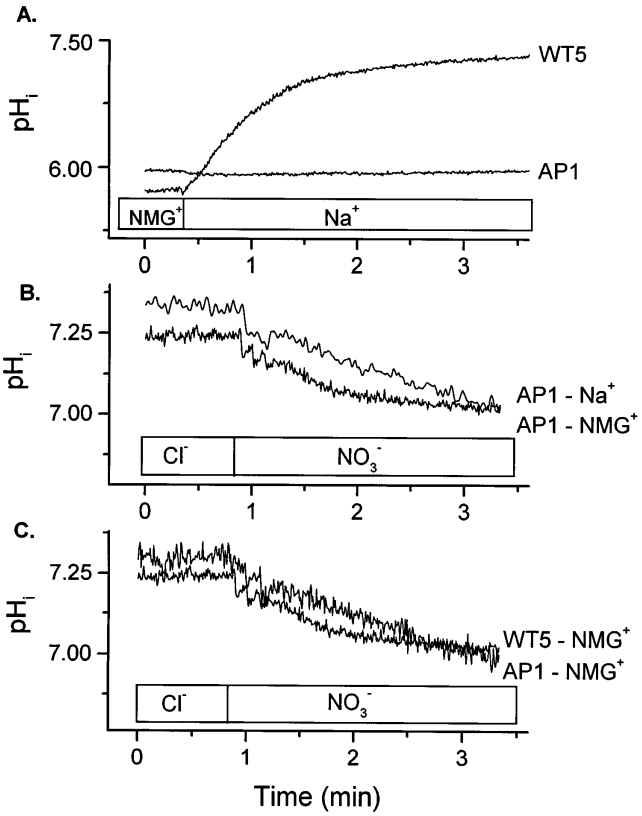

FIGURE 3. NO_3^--induced cytosolic acidification is independent of Na^+/H^+ exchange. (*A*) CHO cells grown to confluence on glass coverslips were loaded with BCECF and used for fluorimetric determination of pH_i. WT5 cells are wild-type CHO cells, while AP1 cells are antiport-deficient CHO mutants isolated by the H^+-suicide technique (see EXPERIMENTAL PROCEDURES). Before the initiation of the trace, the cells were acid loaded by means of an ammonium pre-pulse (25 mM for 10 min). The trace starts upon perfusion of the ammonium-loaded cells with a Na^+-free, NMG-Cl solution (pH 7.5). Where indicated, the bathing medium was switched to a Na^+-rich solution (NaCl, pH 7.5). Representative of 5 experiments. (*B* and *C*) pH_i was measured fluorimetrically in CHO cells loaded with BCECF, as in panel *A*. In *B* AP1 cells were perfused initially with NaCl or NMG-Cl medium, as indicated. Where noted, the media were changed to $NaNO_3$ or NMG-NO_3 solution, respectively. In *C* WT5 (*top trace*) or AP1 cells (*lower trace*) were perfused initially with NMG-Cl medium. Where noted, the perfusing medium was switched to NMG-NO_3 solution. Traces in *B* and *C* are representative of 6 experiments, respectively. Mean NO_3^--induced H^+ flux of AP-1 cells was 2.54 ± 0.40 mmol/liter/min in Na^+-rich solution and 2.22 ± 0.45 mmol/liter/min in NMG^+-rich solution. Mean NO_3^--induced H^+ flux of WT5 cells in NMG^+-rich solution was 2.39 ± 0.39 mmol/liter/min.

ited by amiloride and its analogues (not shown), is the hallmark of NHE activity. By contrast, AP1 cells failed to recover when Na^+ was reintroduced to the perfusate, implying that they are devoid of NHE.

Despite the absence of NHE, AP1 cells exhibited a cytosolic acidification upon addition of external NO_3^-. The rate and extent of acidification were similar in the presence and absence of extracellular Na^+ (Fig. 3 *B*). The mean NO_3^--induced H^+ flux was 2.54 ± 0.40 mmol/liter/min ($n = 6$) in Na^+-rich solution and 2.22 ± 0.45 mmol/liter/min in NMG^+-rich solution ($n = 6$). These observations imply that NHE is not essential for NO_3^- to induce cytosolic pH changes.

Furthermore, NO_3^--induced cytosolic acidification was observed in wild-type CHO cells bathed in the absence of external Na^+ (mean NO_3^--induced H^+ flux in NMG^+-rich solution was 2.39 ± 0.39 mmol/liter/min; $n = 6$). Under these conditions, forward NHE activity is abrogated and only backward exchange can occur, which can lead to cytosolic acidification. Inhibition of this process by NO_3^- would be expected to have the converse effect, namely, cytosolic alkalinization. However, as shown in Fig. 3 *C*, NO_3^- produced an acidification in WT5 cells that was indistinguishable from that noted in AP1 cells. Together, the data using ion substitution and genetic deletion of the antiporter indicated that the NO_3^--induced cellular acidification is not mediated by inhibition of NHE.

NO_3^--induced Cytosolic Acidification Is Not Mediated by the Anion Exchanger

The Cl^-/HCO_3^- exchanger has affinity for other anions, including NO_3^- (see Cabantchik and Greger, 1992; Reinertsen et al., 1989 for review), and NO_3^-/HCO_3^- exchange has been reported (Kemp and Boyd, 1993; Humphrey et al., 1994; Zhao et al., 1994). Though our experiments were conducted in the nominal absence of HCO_3^-, we cannot a priori exclude the possibility that exchange of cellular HCO_3^- for external NO_3^- accounts for the acidification, particularly considering the finding that DIDS inhibited a sizable fraction of NO_3^- uptake. To address this possibility directly, the effect of NO_3^- on pH_i was measured in the presence of DIDS. As shown in Fig. 4 *A*, the NO_3^--induced acidification persisted when WT5 cells were treated with 100 μM DIDS. The $H^+_{(equivalent)}$ flux in control cells was 2.5 ± 0.5 mmol/liter/min and 2.7 ± 0.5 mmol/liter/min for DIDS treated cells ($n = 4$). No effect on the rate of cytosolic acidification was found using up to 1 mM of DIDS for 15 min (results not shown).

To further assess the role of the anion exchanger in the NO_3^--induced pH changes, we tested a human embryonic kidney (HEK) cell line which has been reported to lack endogenous Cl^-/HCO_3^- exchange activity (Lee et al., 1991). As shown in Fig. 4 *B*, perfusion of

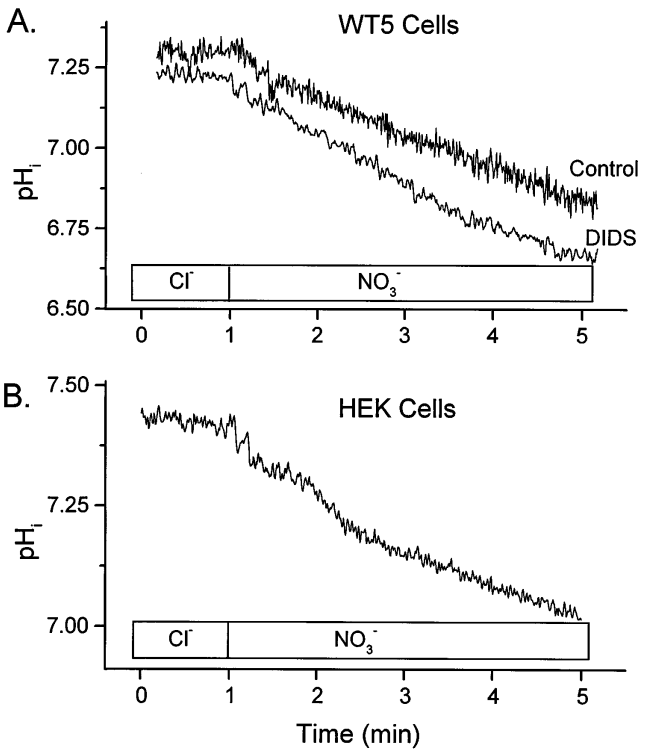

FIGURE 4. NO_3^--induced cytosolic acidification is independent of the anion exchanger. (*A*) pH_i was measured fluorimetrically in CHO cells (WT5) loaded with BCECF. The cells were perfused initially with NMG-Cl medium and, where noted, the perfusing medium was switched to NMG-NO_3 solution. For the lower trace the cells were pre-treated with 100 μM DIDS for 2 min before the initiation of the trace and the same concentration of the stilbene was present throughout the measurement period illustrated. (*B*) Microfluorimetric measurement of pH_i in HEK cells. The cells were initially bathed in NMG-Cl solution and, where indicated, the medium was switched to NMG-NO_3 solution. Traces in *A* and *B* are representative of 6 experiments, respectively.

HEK cells with external NO_3^- promoted a robust acidification, at a rate that was in fact greater than that observed in CHO cells (Table I). Jointly, these data suggest that the anion exchanger is not responsible for the NO_3^--induced cytosolic acidification.

NO_3^--induced Cytosolic Acidification Is Not Mediated by the V-ATPase

The V-ATPase, a H^+-pump whose primary function is acidification of intracellular organelles (see Gluck, 1993 for review), also plays a role in the homeostasis of pH_i in some cell types (Swallow et al., 1991). In osteoclasts as well as in organelles studied in vitro, NO_3^- has been reported to inhibit the V-ATPase (Chatterjee et al., 1993; Dschida and Bowman, 1995). Because the V-ATPase continuously removes H^+ from the cytosol, inhibition of this enzyme by NO_3^- could result in acidification. Two approaches were used to evaluate this possibility. In the first, the pump was inhibited by de-

pleting cells of ATP by inhibiting glycolysis and oxidative phosphorylation using 2-deoxy-D-glucose and antimycin A. In CHO cells this results in depletion of >90% of the cellular ATP within 10 min (determined using luciferin-luciferase; Goss et al., 1994). As illustrated in Figs. 5, *A* and *B*, such ATP-depleted cells exhibited cytosolic acidification when exposed to extracellular NO_3^-. The mean H^+ flux of ATP-depleted cells was comparable to that of control cells (2.38 ± 0.31 mmol/liter/min and 2.03 ± 0.42 mmol/liter/min, respectively; $n = 4$).

A second approach to evaluate the possible role of the V-ATPase used bafilomycin A_1, a macrolide antibiotic which is a potent and specific inhibitor of the pump (Crider et al., 1994; Zhang et al., 1994). In these experiments, WT5 cells were pre-incubated for 2 min in a Cl^--rich, NO_3^--poor solution, with 50 nM bafilomycin, a concentration shown previously to fully inhibit V-ATPases in a variety of cell types (Zhang et al., 1994; Crider et al., 1994). Subsequently, pH_i was microfluorimetric measured upon exposure of cells to isotonic NO_3^--rich solution. Comparison of four experiments in bafilomycin-treated cells with their respective controls revealed no differences in $H^+_{(equivalent)}$ flux (1.46 ± 0.41 and 1.42 ± 0.32 mmol/liter/min in control and bafilomycin-treated cells, respectively; Fig. 5 *B*). Jointly, the results of the ATP depletion and bafilomycin studies suggest that the NO_3^--induced cytosolic acidification is not mediated by the inhibition of the V-ATPase. Furthermore, the NO_3^--induced cytosolic acidification appears to be an ATP-independent process.

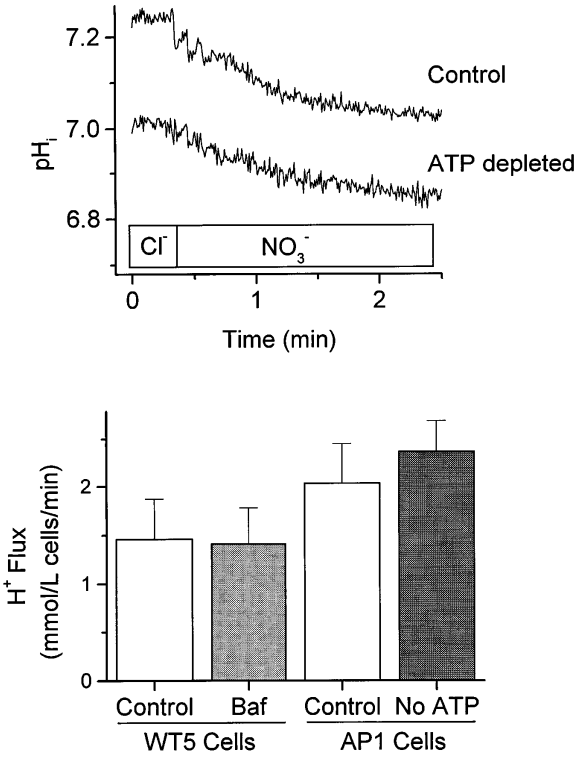

FIGURE 5. NO_3^--induced cytosolic acidification is independent of the V-ATPase. (*A*) pH_i was measured fluorimetrically in CHO cells (AP1) loaded with BCECF. The cells were perfused initially with NMG-Cl medium and, where noted, the perfusing medium was switched to NMG-NO_3 solution. For the lower trace the cells had been ATP depleted by preincubation for 10 min in glucose-free solution with 5 mM 2-deoxy-D-glucose and 1 μg/ml antimycin A. The fluorescence measurements were performed in glucose-free solutions. Traces are representative of 4 determinations. (*B*) Quantitation of the NO_3^--induced cytosolic acidification in CHO cells. (*left*) WT5 cells. Where specified (*stippled bar*), the cells were treated with 50 nM bafilomycin for 2 min before, and also during the pH_i measurements in KCl or KNO_3 solutions. (*right*) AP1 cells. Where specified (*stippled bar*), the cells were ATP depleted as above. The pH_i measurements were performed in NMG-Cl and NMG-NO_3 solutions. $H^+_{(equivalent)}$ flux was calculated by multiplying the rate of pH_i change ($\Delta pH_i/\Delta time$) by the buffering capacity of CHO cells, measured to be 25 mmol/pH/liter of cells in the pH range of our measurements (Kapus et al., 1994). Data are means ± SE of 4 determinations.

Possible Role of NO_2^- and Other Nitrogen Oxides in NO_3^--induced Cytosolic Acidification

Solutions of NO_3^- can contain small amounts of NO_2^- and/or other nitrogen oxides. Of relevance, addition of NO_2^- to pancreatic acinar cells was recently shown to induce a sizable cytosolic acidification (Zhao et al., 1994). This pH change was attributed, to a small extent, to the generation and permeation of HNO_2, a weak acid with pK_a of 3.2. The majority of the acidification, however, was seemingly due to the reaction between poorly defined nitrogen oxides (possibly NO, N_2O_3, and/or N_2O_4, intermediates in the oxidation of NO_2^- to NO_3^-) and intracellular H_2O or OH^-. In acinar cells, the latter reaction was found to be catalyzed by carbonic anhydrase (Zhao et al., 1994). These observations raised the possibility that a similar mechanism might underlie the NO_2^--induced acidification in CHO cells. Experiments designed to explore this possibility are illustrated in Fig. 6. The effect of NO_2^- on pH_i was compared with that of acetate, another weak acid with somewhat higher pK ($pK_a = 4.7$). Acetate produced a rapid acidification, as expected from the permeation of the uncharged protonated species, acetic acid. An equimolar concentration of NO_2^- induced a somewhat smaller and slower acidification (−0.27 ± 0.05 pH U/min; $n = 3$), consistent with the >10-fold lower concentration of the protonated species. In both cases, the pH_i changes were rapidly reversed upon removal of the weak acids.

To determine whether nitrogen oxides contributed to the acidification by a carbonic anhydrase-mediated process, the cells were treated with methazolamide, an inhibitor of the anhydrase. A representative experiment is shown in Fig. 6 *B*. Neither the rate nor the extent of the NO_2^- -induced acidification were noticeably altered by methazolamide (ΔpH_i = −0.27 ± 0.05 in

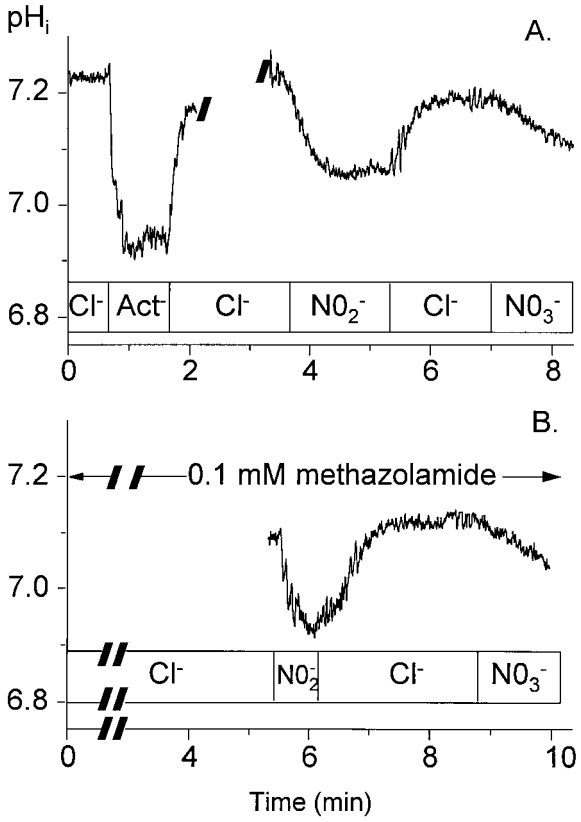

FIGURE 6. Comparison of the effects of $NO_3^-$and NO_2^- on pH_i and assessment of the role of carbonic anhydrase. (*A*) pH_i was measured fluorimetrically in CHO cells (AP1) loaded with BCECF. The cells were perfused initially with 117 mM NaCl medium and, where noted, with solutions containing 10 mM sodium acetate (Act^-), 10 mM $NaNO_2$ or 117 mM $NaNO_3$. The sodium acetate and $NaNO_2$ solutions were osmotically balanced with 107 mM Na-gluconate. (*B*) AP1 cells were preincubated for 5 min with 0.1 mM methazolamide in NaCl solution before fluorimetric measurement of pH_i. Where noted, cells were perfused with solutions containing 10 mM $NaNO_2$ or 117 mM $NaNO_3$, as described in panel *A*, supplemented with 0.1 mM methazolamide. Traces in *A* and *B* are representative of 4 experiments each.

control cells and -0.29 ± 0.07 in cells treated with methazolamide; $n = 3$). Similarly, the more gradual acidification induced by NO_3^- was unaffected by inhibition of carbonic anhydrase ($\Delta pH_i = -0.11 \pm 0.03$ in control cells and -0.10 ± 0.04 in cells treated with methazolamide; $n = 3$). Thus, it appears that H^+ release by reaction of nitrogen oxides with H_2O or OH^- is not an important component of the NO_2^- or NO_3^- response in CHO cells.

To ensure that the NO_3^--induced acidification observed in CHO cells was not due to reduction of extracellular NO_3^- to NO_2^-, the NO_2^- content of solutions containing 29 to 117 mM NO_3^- was measured using the Greiss method (as described in EXPERIMENTAL PROCEDURES). NO_2^- content in the solutions was found to be negligible (mean $[NO_2^-] = 0.44 \pm 0.05$ μM, $n = 8$). Similarly, intracellular NO_2^- levels were found to be negligible up to 10 min after exposure to extracellular NO_3^- (results not shown). Jointly, these results suggest that neither permeation of HNO_2 nor metabolism of contaminating nitrogen oxides are responsible for the acidification induced by NO_3^-.

Properties of the NO_3^--induced H^+ Flux

The results summarized above confirmed that the pH changes promoted by NO_3^- are not due to modulation of the predominant homeostatic pathways and are accompanied by transport of NO_3^- across the membrane. The simplest model to explain the effects of the anion is therefore the cotransport of NO_3^- with H^+, or its equivalent, NO_3^-/OH^- counter-transport. For simplicity, and by analogy with the system described in plants and fungi (Downey and Gedeon, 1994; Mehrag and Blatt, 1995), we will tentatively assume hereafter that NO_3^--H^+ cotransport is responsible for the observed pH_i changes.

The kinetic properties of the putative NO_3^--H^+ cotransport were investigated next. The extracellular $[H^+]$ dependence was determined in AP1 cells suspended in $NaNO_3$ solutions titrated between pH 6.0 to 7.5. Because reducing the extracellular pH (pH_o) is expected to reduce pH_i by pathways other than the NO_3^--H^+ cotransporter, the NO_3^--independent component of the pH change was also measured by perfusing the cells in NaCl solution titrated to the appropriate pH. The NO_3^--independent H^+ flux at pH 6.0, 6.5, and 7.0 was 4.11 ± 0.88, 1.71 ± 0.93, and 1.36 ± 0.77 mmol/liter/min, respectively. The NO_3^--independent component was then subtracted from the total change recorded in the presence of NO_3^- at an identical pH_o. The results of these determinations are illustrated in Fig. 7. Increasing external $[H^+]$ in the pH 7.5–6.0 range increased the rate of NO_3^--induced cytosolic acidification, consistent with NO_3^--H^+ cotransport. More extreme levels of pH_o were not studied for fear of inducing cell damage. In the range studied, the half maximal rate of acidification was attained at $[H^+] = 0.09 \pm 0.01$ μM.

To assess the external NO_3^- concentration ($[NO_3^-]_o$) dependence of the putative cotransporter, pH_i was measured in AP1 cells perfused with isotonic solutions containing 3.65–117 mM NO_3^-. These experiments were performed at both pH_o 6.5 and 7.5, and the solutions were osmotically balanced with $gluconate^-$ since this anion was shown earlier to have no discernible effect on pH_i (Fig. 1 *A*). The rate of $H^+_{(equivalent)}$ flux increased with increasing external NO_3^- concentration at both pH_o. The apparent NO_3^- affinity and maximal velocity of the putative cotransporter can be inferred by fitting the data with an Eadie-Hofstee plot (Fig. 8). At pH_o 7.5, V_{max} and K_m were 5.81 ± 0.58 mmol/liter/min

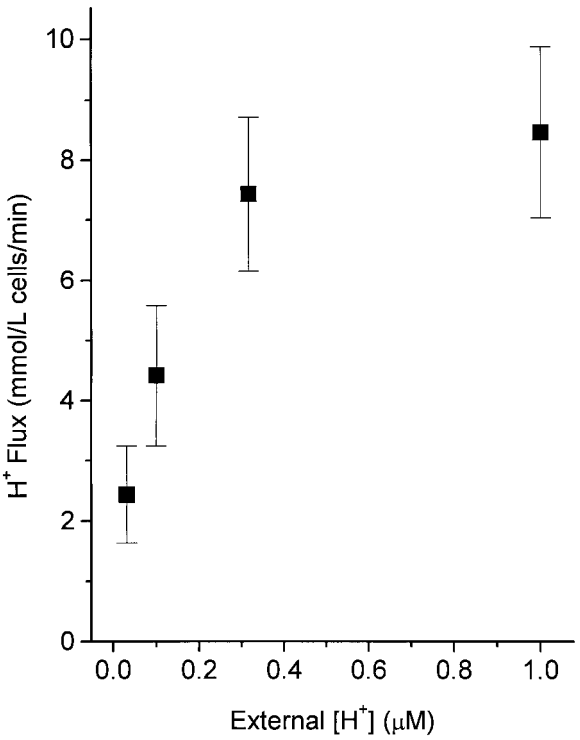

FIGURE 7. External pH dependence of the NO_3^--induced cytosolic acidification. pH_i was measured fluorimetrically in CHO cells (AP1) loaded with BCECF. The pH_i change was measured upon introduction of a NO_3^--rich solution of the indicated external $[H^+]$ (corresponding to a pH_o range of 6.0–7.5). The rate of pH_i change was estimated over a 60 s period and the $H^+_{(equivalent)}$ flux was calculated as in Fig. 5. The NO_3^--independent acidification, due solely to the reduction in extracellular pH was estimated using Cl^--rich solutions of identical pH, and was subtracted from the equivalent measurements performed in NO_3^--rich media (see EXPERIMENTAL PROCEDURES). NO_3^--independent H^+ flux at pH_o of 6.0, 6.5, 7.0 was 4.11 ± 0.88, 1.71 ± 0.93 and 1.36 ± 0.77 mmol/liter/min, respectively. Data are means ± SE of 5 experiments.

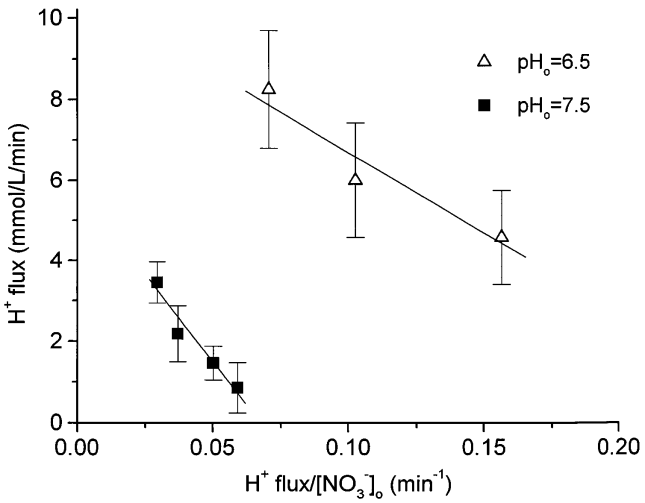

FIGURE 8. NO_3^- concentration dependence: Eadie-Hofstee plot. pH_i was measured fluorimetrically in CHO cells (AP1) loaded with BCECF. The cells were equilibrated in Cl^--rich medium and pH_i changes were measured upon introduction of solutions of varying NO_3^- concentration (from 6.65 to 117 mM). The solutions were osmotically balanced using gluconate. No significant pH_i change was induced by gluconate itself (e.g., Fig. 1). The rate of pH_i change was estimated over a 60 s period and the $H^+_{(equivalent)}$ flux was calculated as in Fig. 5. These experiments were performed at pH_o = 7.5 (*closed squares*) and pH_o = 6.5 (*open triangles*). Data are means ± SE of 4 determinations. V_{max} and K_m, derived by linear regression from the Eadie-Hofstee plot were 5.8 ± 0.6 mmol/liter/min and 86.2 ± 12.6 mM for pH_o = 7.5 (R = −0.98) and 10.7 ± 1.3 mmol/liter/min and 40.1 ± 10.6 mM for pH_o = 6.5 (R = −0.97).

and 86.2 ± 12.6 mM, respectively (R = −0.98). At pH_o 6.5, V_{max} and K_m were 10.7 ± 1.3 mmol/ liter/min and 40.1 ± 10.6 mM, respectively (R = −0.97). Because the apparent affinity of the transporter for NO_3^- is modified by $[H^+]_o$, we conclude that binding of the ions to the transporter cannot occur independently in random order. The altered affinity is consistent with an allosteric effect of protons on the conformation of the NO_3^- binding site(s).

Effect of Monovalent Cations on NO_3^--induced Cytosolic Acidification

Some anion transporters are cation dependent (Roos and Boron, 1981; Schron et al., 1985; Shrode et al., 1995). To assess whether cationic species affect the rate of NO_3^--induced cytosolic acidification, pH_i was measured in isotonic NO_3^--rich solutions containing Na^+, K^+, or NMG^+ as the principal cation. The cells were initially equilibrated with Cl^--rich solutions of the same cationic composition and then switched to NO_3^- media. AP1 cells were used for these measurements to eliminate possible confounding effects due to NHE. As summarized in Table II, no statistically significant differences in rate of H^+ flux were observed in K^+ or NMG^+ solutions when compared with Na^+ solutions.

TABLE II

Cationic Dependence of NO_3^--induced Acidification

	$H^+_{(equivalent)}$ flux	*n*	*P* (vs. Na^+)
	mmol/liter cells/min		
Na^+	2.54 ± 0.40	6	N/A
NMG^+	2.22 ± 0.45	6	0.58
K^+	1.88 ± 0.37	6	0.18

AP1 cells grown on coverslips were loaded with BCECF and used for microfluorimetric measurement of pH_i, as described under METHODS. The cells wre perfused sequentially with NaCl, $NaNO_3$, NMG-Cl, NMG-NO_3, KCl, and KNO_3 solutions (pH 7.5), so as to compare the initial rates of NO_3^--induced acidification induced by each cation in the same coverslip at comparable starting pH_i. The composition of the media is detailed in METHODS. All experiments were performed at 37°C. Data are means ± one standard error. *P*-values, calculated using Student's *t* test, compare the effects vs. Na^+. NMG^+ = *N*-methyl-D-glucammonium$^+$.

Voltage Sensitivity of the NO_3^--induced Cytosolic Acidification

The DIDS-insensitive rate of NO_3^- influx into AP1 cells was 2.66 ± 0.07 mmol/liter/min (Fig. 2). Under comparable experimental conditions, the rate of $H^+_{(equivalent)}$ flux was calculated to be 2.63 ± 0.99 mmol/liter/min (Table III). The apparent stoichiometry of the putative NO_3^--H^+ cotransporter derived from these flux rates is therefore one-to-one. This calculation assumes that all the stilbene-insensitive NO_3^- flux is coupled to H^+ transport, a premise that has not been validated experimentally. An alternative approach to estimate the stoichiometry of the cotransport process is to analyze its voltage sensitivity. An electroneutral one-to-one exchanger is likely to be voltage insensitive, whereas changes in voltage are more likely to affect a transporter with unequal stoichiometry.

To gain further insight into the mechanism of NO_3^--H^+ cotransport, we evaluated its electrical properties in cells patch-clamped in the whole cell configuration. We estimated that it would be difficult to measure a current mediated by the transporter, since this was calculated to be as low as 4.2 or 8.4 pA if assuming a stoichiometry of 2:1 or 3:1, respectively. Instead, we assessed whether the NO_3^--induced pH_i changes would be affected by drastic changes in the membrane potential. A pipette solution with low buffering capacity (1 mM MES) was used to maximize the NO_3^--induced pH_i changes. A representative pH_i measurement in a voltage-clamped cell is shown in Fig. 9. The cell was initially clamped at −60 mV and superfused with a Cl^--rich solution. Under these conditions, pH_i was unaffected by a sudden depolarization to 0 mV, confirming that CHO cells have a comparatively low $H^+_{(equivalent)}$ conductance at physiological pH_i and at normal resting membrane potential (Demaurex et al., 1995). Cytosolic acidification was observed when NO_3^- replaced Cl^- in the bathing solution. The occurrence of an acidification in voltage clamped cells implies that the effect of NO_3^- on pH_i is not mediated by, and does not require changes in membrane potential. Moreover, the rate of pH_i change was not affected by sequentially stepping the membrane potential up from −60 to +40 mV; only the normal exponential decay was noted. A comparable decay was observed when the order of the voltage changes was reversed, from depolarized to repolarized (not illustrated). The data in patch clamped cells indicate that the NO_3^--induced cytosolic acidification is voltage insensitive, consistent with an electrically neutral process. This conclusion is compatible with the tentative estimates of stoichiometry of one-to-one.

TABLE III

Effects of Pharmacological Agents on the Rate of NO_3^--induced Cytosolic Acidification

	$H^+_{(equivalent)}$ flux (mmol/liter cells/min)	%	*n*	*P* (*vs. control*)
Control	3.06 ± 0.43	100%	19	N/A
Ethacrynic acid (100 μM)	1.01 ± 0.48	33%	4	0.07
CHC (1 mM)	0.62 ± 0.49	20%	4	0.03
pCMBS (250 μM)	2.00 ± 0.36	65%	4	0.35
Phloretin (100 μM)	3.79 ± 1.56	124%	4	0.61
DIDS (100 μM)	2.63 ± 0.99	86%	6	0.65
ATP depletion	2.38 ± 0.31	76%	5	0.40
Methazolamide (0.1 mM)	2.48±1.01	81%	3	0.68

NO_3^--induced acidification was measured in BCECF-loaded AP1 cells upon transfer from NaCl to $NaNO_3$ solution or, in the case of ATP-depleted cells, from NMG-Cl to NMG-NO_3. Cells were preincubated with the following inhibitors for the specified period of time: 100 μM DIDS for 2 min, 1 mM CHC for 5 min, 100 μM ethacrynic acid for 10 min, 250 μM pCMBS for 10 min, 100 μM phloretin for 10 min, and 0.1 mM methazolamide for 5 min. DIDS, CHC, phloretin and methazolamide were also present during the measurement. For ATP depletion, cells were incubated for 10 min in glucose-free medium with 5 mM deoxyglucose and 1 μg/ml antimycin A to inhibit both glycolysis and oxidative phosphorylation. Subsequent fluorescence measurements were performed in glucose-free mdedium containing containing 5 mM deoxyglucose. All procedures were performed at 37°C. Data are means ± standard error of the indicated number of experiments. *P* was calculated using Student's paired *t* test. CHC = α-cyano-4-hydroxycinnamate, DIDS = 4,4′-diisothiocyanostilbene-2,2′ disulfonate, NMG = *N*-methyl-D-glucammonium$^+$, pCMBS = *p*-chloromercuribenzene.

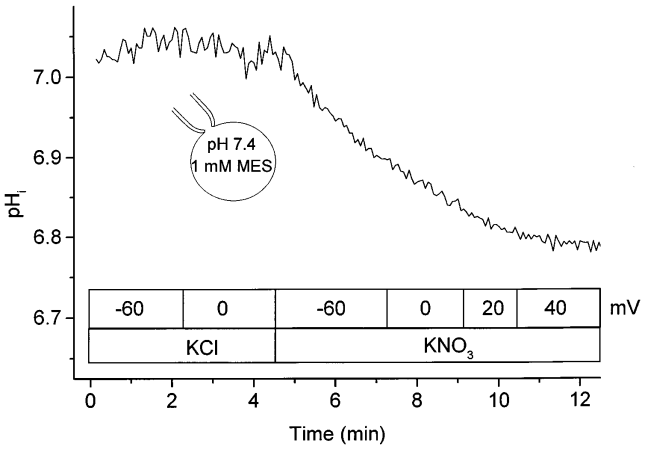

FIGURE 9. Effect of membrane potential on NO_3^--induced cytosolic acidification. An AP1 cell was voltage clamped in the whole-cell configuration of the patch-clamp technique, using a pipette filled with low buffer, KCl-rich solution containing BCECF. pH_i was measured microfluorimetrically on the photometric system described in METHODS. Over 5 min were allowed at a holding potential of −60 mV for adequate fluorophore loading and for equilibration of the cytosol with the pipette solution before initiation of the pH measurements. The cell was initially superfused with KCl solution and subsequently with KNO_3 solution, as noted. The holding voltage was stepped to values ranging from −60 mV to +40 mV, as indicated. Representative of 4 similar experiments.

Effect of Inhibitors on the NO_3^--induced Cytosolic Acidification

To establish possible analogies with other mammalian transporters, we tested a variety of compounds known to inhibit other plasmalemmal ion transport systems. Ethacrynic acid (Poole and Halestrap, 1993; Koechel, 1981; Palfrey and Leung, 1993), a dichlorophenoxyacetic acid derivative, is a potent alkylating reagent that has loop diuretic action. It is known to inhibit several ion carriers, including the $Na^+/K^+/Cl^-$ cotransporter (Palfrey and Leung, 1993). NO_3^--induced cytosolic acidification was 67% inhibited by 100 μM ethacrynic acid (Table III). The mean $H^+_{(equivalent)}$ flux in ethacrynic acid treated-cells was 1.01 ± 0.48 mmol/liter cells/min ($n = 4$) compared with 3.06 ± 0.43 mmol/ liter cells/min in paired controls ($n = 19$). Inhibition by ethacrynic acid was almost complete at 200 μM (not shown).

α-Cyano-4-hydroxycinnamate (CHC) inhibits both the anion exchanger (Simchowitz, 1988) and the monocarboxylate transporter (Poole and Halestrap, 1993) in other cells. CHC (1 mM) inhibited NO_3^--induced cytosolic acidification to 20% of the control rate (Table III). $H^+_{(equivalent)}$ flux in CHC-treated cells was 0.62 ± 0.49 mmol/liter cells/min ($n = 4$).

Phloretin, the aglycone of phlorizin, is a reversible, relatively nonspecific inhibitor of several membrane transport processes, including urea transport, monocarboxylate transport and Cl^-/HCO_3^- exchange (Wang et al., 1993; Melnik et al., 1977; Chou and Knepper, 1989). In our experiments, 100 μM phloretin was found to have no effect on the rate of NO_3^--induced cytosolic acidification (Table III).

pCMBS, an organomercurial sulfhydryl reagent, irreversibly inhibits the monocarboxylate transporter (Munzel et al., 1995) but does not affect the Cl^-/HCO_3^- exchanger (Poole and Halestrap, 1993; Zhang and Solomon, 1992). NO_3^--induced cytosolic acidification was unaffected by 250 μM pCMBS (Table III). Similarly, NO_3^--induced cytosolic acidification was not affected by furosemide (data not shown), a loop diuretic that inhibits several anion transport systems, including the Cl^-/HCO_3^- exchanger (Cabantchik et al., 1978), the monocarboxylate transporter (Poole and Halestrap, 1993) and the SO_4^{2-}/OH^- exchanger (Schron et al., 1985) which is reportedly distinct from the SO_4^{2-}/Cl^- exchanger (Schron et al., 1987).

In summary, though the NO_3^--induced H^+ transporter shares some properties with the monocarboxylate transporter and anion exchange systems, it appears to be a pharmacologically distinct entity.

DISCUSSION

A rapid, reversible cytosolic acidification was detected upon exposure of the cells to solutions that were rich in NO_3^-. The acidification was detected by both photometry and ratio imaging, and was eliminated when ionophores were used to clamp pH_i or when the buffering power of the cytosol was increased greatly by intracellular perfusion with heavily buffered solutions. Together, these observations imply that NO_3^- produces a veritable change in cytosolic pH. It is noteworthy that, in isolated perfused rat heart, NO_3^- was similarly found to reduce intracellular pH, an effect which was exacerbated by ischemia (Curtis et al., 1993).

The pH_i changes elicited by NO_3^- were seemingly not due to modulation of the activity of other, known acid/base transport systems. Briefly, the NO_3^--induced acidification persisted in Na^+-free solutions and was also observed in cells devoid of Na^+/H^+ antiporter, ruling out a requirement for this transporter. Similarly, the effects of NO_3^- were still observable in the nominal absence of HCO_3^- and in the presence of stilbene disulfonates, and were also displayed by HEK 293 cells, which are reportedly devoid of anion exchangers (Lee et al., 1991). Thus, both cation-independent and Na^+-dependent anion exchange are unlikely to mediate the effects of NO_3^-. Finally, though sensitive to NO_3^-, vacuolar-type H^+ pumps are not involved in the observed effects of the anion on pH_i. This was concluded because the NO_3^--induced acidification persisted in cells treated with bafilomycin at concentrations that fully inhibit the vacuolar pumps (Chatterjee et al., 1993; Dschida and Bowman, 1995).

Studies in pancreatic acinar cells have indicated that NO_2^- and/or other nitrogen oxide species mediate intracellular acidification by reacting with H_2O or OH^- in a carbonic anhydrase catalyzed process (Feldman, 1994). This mechanism is unlikely to account for the NO_3^--induced pH changes observed in CHO cells since: (*a*) the acidification was insensitive to carbonic anhydrase inhibitors (Fig. 6 and Table III). In fact, the NO_2^--induced acidification in CHO cells was also insensitive to methazolamide, suggesting that the metabolism of nitrogen oxides observed in pancreatic acinar cells is not a universal process; (*b*) only traces of NO_2^- were found in our NO_3^- solutions. In our hands, the acidification induced by NO_2^- can be largely explained by permeation of HNO_2. The pH change recorded is close to that predicted on the basis of the pK of the acid and the buffering power of the cells. Thus, we found no evidence for significant conversion of NO_3^- to more reduced nitrogen oxides or for a role of the latter in the acidification. Nevertheless, we cannot rule out the possibility that such contaminants are present or generated during the course of the experiment and that they may contribute to the pH changes.

Finally, the acidification induced by NO_3^- may have resulted from increased metabolic acid generation. We consider this unlikely for two reasons. First, the effect

of NO_3^- was largely unaffected by metabolic depletion of the cells using deoxyglucose and antimycin. Secondly, the magnitude of the acidification was proportional to the extracellular concentration of H^+ (Fig. 7). Jointly, these observations suggest that NO_3^- drives the transmembrane flux of H^+ equivalents through a nonconventional system.

NO_3^- was taken up by the cells during the course of the pH_i changes, supporting the notion that carrier-mediated cotransport occurred. Accordingly, the uptake of NO_3^- was saturable and the accompanying pH_i changes displayed anion selectivity and susceptibility to inhibition by agents that block other transporters. Though the fraction of the uptake of nitrate mediated by the putative cotransporter could not be defined precisely, a coarse stoichiometry could be approximated, assuming that the stilbene-insensitive component is fully engaged in $H^+_{(equivalent)}$ transport. The calculated stoichiometry of approximately 1 to 1 is consistent with the finding that the acidification induced by NO_3^- was unaffected by changes in the membrane potential (Fig. 9). The cumulative evidence can therefore be most simply explained by proposing the existence of an electroneutral cotransport of NO_3^- and H^+ (or the equivalent exchange of NO_3^- for OH^-).

Counter-transport of inorganic anions for OH^- or HCO_3^- (Lee et al., 1991; Jiang et al., 1994; Reinertsen et al., 1989; Sheu et al., 1995; Begault and Edelman, 1993) and organic anion for HCO_3^- (Kuo and Aronson, 1988) have, of course, been extensively studied. However, the present system appears to differ from other transporters described earlier (Sheu et al., 1995; Kuo and Aronson, 1988; Simchowitz, 1988) in that it appears to be rather insensitive to stilbene disulfonates and transports NO_3^- more avidly than Cl^-. Divalent inorganic anions such as SO_4^{2-} can be cotransported with H^+ in exchange for a monovalent anion through the anion exchanger (Schron et al., 1987), yet this process is also unlikely to mediate the observed effects of NO_3^-, given its insensitivity to stilbenes. Moreover, cotransport of NO_3^- and H^+ in exchange for a monovalent anion would be rheogenic and most likely potential sensitive, unlike the electroneutral process described here.

Both functionally and pharmacologically, the putative NO_3^--H^+ transporter resembles most closely the properties of the organic acid-H^+ cotransport system (Poole and Halestrap, 1993; Wang et al., 1993; Jackson and Halestrap, 1996). Both are sensitive to CHC and to ethacrynic acid. Yet, unlike the NO_3^--induced acidification, the monocarboxylate-H^+ cotransporter is inhibited by DIDS, phloretin and pCMBS (Poole and Halestrap, 1993). Thus, these systems appear to be distinct, though possibly related.

Though, to our knowledge, NO_3^--H^+ cotransport had not been reported in mammalian cells, comparable systems have in fact been described and well characterized in *Arabidopsis thalia* and in *Aspergillus nidulans* (Downey and Gedeon, 1994; Mehrag and Blatt, 1995). In fact, the gene encoding the transporter of *Arabidopsis* (termed CHL1) has been cloned (Tsay et al., 1993) and found to have sequence homology to the amino acid transporter, NTR1, of the same organism (Rentsch et al., 1995). Nevertheless, the stoichiometry and voltage-sensitivity profile of the plant (Tsay et al., 1993; Mehrag and Blatt, 1995) and fungal (Downey and Gedeon, 1994) NO_3^--H^+ cotransporter differ from those described here for mammalian cells. The cotransporters of lower organisms are rheogenic and voltage sensitive (Downey and Gedeon, 1994; Tsay et al., 1993; Mehrag and Blatt, 1995) and when measured, the transport stoichiometry of the plant NO_3^--H^+ cotransporter was found to be 1 NO_3^-:2 H^+ (Mehrag and Blatt, 1995). Though not identical, the plant and fungal transporters may be related to their mammalian counterpart and may provide useful tools for the identification of the cotransporter described here. Low stringency hybridization or PCR using conserved coding sequences of the CHL1 gene may serve to identify the equivalent mammalian gene.

Regardless of the precise molecular identity of the putative cotransporter, it is evident that mammalian cells have efficient NO_3^- transport mechanisms and these may be important in eliminating the products of NO metabolism, particularly in cells that generate vast amounts of this mediator. That the transporter operates in both a forward and reverse direction is likely of importance for the transport of NO_3^- across different tissue beds before disposal in the genitourinary and/or gastrointestinal tracts. Furthermore, the occurrence of NO_3^--H^+ cotransport would offer the added advantage of eliminating acid equivalents from cells that are metabolizing actively, without added energetic investment and without disruption of the transmembrane potential, inasmuch as the cotransporter is likely electroneutral.

The authors gratefully acknowledge the thoughtful comments of Mr. Mehrdad Yazdanpanah and Dr. Graham Ellis regarding the measurement of intracellular nitrate, and those of Dr. Nicolas Demaurex during the preparation of the manuscript.

This work is supported by the Medical Research Council of Canada. C.W. Chow is the recipient of a Clinician-Scientist Award from the Department of Medicine, Faculty of Medicine, University of Toronto. S. Grinstein is an International Scholar of the Howard Hughes Medical Institute.

Original version received 28 January 1997 and accepted version received 3 June 1997.

REFERENCES

Anggard, E. 1994. Nitric oxide: mediator, murderer and medicine. *Lancet.* 343:1199–1206.

Begault, B., and A. Edelman. 1993. A nucleotide-regulated Cl^-/OH^- anion exchanger in endoplasmic reticulum-enriched pig pancreatic microsomes. *Biochim. Biophys. Acta.* 1146:183–190.

Bruce, L.J., D.J. Anstee, F.A. Spring, and M.J.A. Tanner. 1994*a*. Band 3 Memphis variant II. *J. Biol. Chem.* 23:16155–16158.

Bruce, L.J., J.D. Groves, Y. Okubo, B. Thilaganathan, and M.J.A. Tanner. 1994*b*. Altered band 3 structure and function in glycophorin A- and B-deficient (M^kM^k) red blood cells. *Blood.* 84:916–922.

Cabantchik, Z.I., P.A. Knauf, and A. Rothstein. 1978. The anion transport system of the red blood cell. *Biochim. Biophys. Acta.* 515:239–302.

Cabantchik, Z.I., and R. Greger. 1992. Chemical probes for anion transporters of mammalian cell membranes. *Am. J. Physiol.* 262:C803–C827.

Chatterjee, D., L. Neff, M. Chakraborty, C. Fabricant, and R. Baron. 1993. Sensitivity to nitrate and other oxyanions further distinguishes the vanadate-sensitive osteoclast proton pump from other vacuolar H^+-ATPases. *Biochemistry.* 32:2808–2812.

Chou, C.L., and M.A. Knepper. 1989. Inhibition of urea transport in inner medullary collecting duct by phloretin and urea analogues. *Am. J. Physiol.* 257:F359–F365.

Crider, B.P., X.-S. Xie, and D.S. Stone. 1994. Bafilomycin inhibits proton flow through the H^+ channel of vacuolar proton pumps. *J. Biol. Chem.* 269:17379–17381.

Curtis, M.J., P.B. Garlick, and R.D. Ridley. 1993. Anion manipulation, a novel antiarrythmic approach: mechanism of action. *J. Mol. Cell. Cardiol.* 25:417–436.

Demaurex, N., J. Orlowski, G. Brissean, M. Woodside, and S. Grinstein. 1995. The mammalian Na^+/H^+ antiporters NHE-1,NHE-2 and NHE-3 are electroneutral and voltage independent, but can couple to an H^+ conductance. *J. Gen. Physiol.* 106:85–111.

Downey, R.J., and C.A. Gedeon. 1994. Evidence for a H^+ nitrate symporter in *Aspergillus nidulans. Microbios.* 78:35–46.

Drobyski, W.R., C.A. Keever, G.A. Hanson, T. McAuliffe, and O.W. Griffith. 1994. Inhibition of nitric oxide production is associated with enhanced weight loss, decreased survival, and impaired alloengraftment in mice undergoing graft-versus-host disease after bone marrow transplantation. *Blood.* 84:2363–2373.

Dschida, W.J.A., and B.J. Bowman. 1995. The vacuolar ATPase: sulfite stabilization and the mechanism of nitrate inactivation. *J. Biol. Chem.* 270:1557–1563.

Feldman, G.M. 1994. HCO_3^- secretion by rat distal colon: effects of inhibitors and extracellular Na^+. *Gastroenterology.* 107:329–338.

Gilliam, M.B., M.P. Sherman, J.M. Griscavage, and L.J. Ignarro. 1993. A spectrophotometric assay for nitrate using NADPH oxidation by Aspergillus nitrate reductase. *Anal. Biochem.* 212:359–365.

Gluck, S.L. 1993. The vacuolar H^+-ATPases: versatile proton pumps participating in constitutive and specialized functions of eukaryotic cells. *Int. Rev. Cyt.* 137:105–137.

Goss, G.G., M. Woodside, S. Wakabayashi, J. Pouyssegur, T. Waddell, G.P. Downey, and S. Grinstein. 1994. ATP dependence of NHE-1, the ubiquitous isoform of the Na^+/H^+ antiporter. Analysis of phosphorylation and subcellular localization. *J. Biol. Chem.* 269:8741–8748.

Green, L.C., D.A. Wagner, J. Glogowski, P.L. Skipper, J.S. Wishnok, and S.R. Tannenbaum. 1982. Analysis of nitrate, nitrite and [^{15}N]nitrate in biological fluids. *Anal. Biochem.* 126:131–138.

Humphrey, B.D., L. Jiang, M.N. Chernova, and S.L. Alper. 1994. Functional characterization and regulation by pH of murine AE2 anion exchanger expressed in *Xenopus* oocytes. *Am. J. Physiol.* 267:C1295–C1307.

Ignarro, L.J. J.M. Fukuto, J.M. Griscavage, N.E. Rogers, and R.E. Byrns. 1993. Oxidation of nitric oxide in aqueous solution to nitrite but not nitrate: comparison with enzymatically formed nitric oxide from l-arginine. *Proc. Nat. Acad. Sci. USA.* 90:8103–8107.

Iyengar, R., D.J. Stuehr, and M.A. Marletta. 1987. Macrophage synthesis of nitrite, nitrate, and n-nitrosamines: precursors and role of the respiratory burst. *Proc. Natl. Acad. Sci. USA.* 84:6369–6373.

Jackson, V.N., and A.P. Halestrap. 1996. The kinetics, substrate and inhibitor specificity of the monocarboxylate (lactate) transporter of rat liver cells determined using the fluorescent intracellular pH indicator, 2′, 7′-bis(carboxylethyl)-5,(6)-carboxyfluorescein. *J. Biol. Chem.* 271:861–868.

Jennings, M.L., S.M. Douglas, and P.E. McAndrew. 1986. Amiloride-sensitive sodium-hydrogen exchange in osmotically shrunken rabbit red blood cells. *Am. J. Physiol.* 251:C32–C40.

Jiang, L., A. Stuart-Tilley, J. Parkash, and S.L. Alper. 1994. pH_i and serum regulated AE2-mediated Cl^-/HCO_3^- exchange in CHOP cells of defined transient transfection status. *Am. J. Physiol.* 267: C845–C856.

Jungersten, L., A. Edlund, L.O. Hafstrom, L. Karlsson, A.S. Petersson, and A. Wennmalm. 1993. Plasma nitrate as an index of immune system activation in animals and man. *J. Clin. Lab. Immunol.* 40:1–4.

Kapus, A., R. Romanek, A.Y. Qu, O.D. Rotstein, and S. Grinstein. 1993. A pH-sensitive and voltage-dependent proton conductance in the plasma membrane of macrophages. *J. Gen. Physiol.* 102: 729–760.

Kapus, A., S. Grinstein, S. Wasan, R. Kandasamy, and J. Orlowski. 1994. Functional characterization of three isoforms of the Na^+/H^+ exchanger stably expressed in Chinese hamster ovary cells. ATP dependence, osmotic sensitivity, and role in cell proliferation. *J. Biol. Chem.* 269:23544–23552.

Kemp, P.J., and C.A. Boyd. 1993. Anion exchange in type II pneumocytes freshly isolated from adult guinea-pig lung. *Pflugers Arch.* 425:28–33.

Kiechle, F.L., and T. Malinski. 1993. Nitric oxide: biochemistry, pathophysiology and detection. *Am. J. Clin. Pathol.* 100:567–575.

Koechel, D.A. 1981. Ethacrynic acid and related diuretics: relationship of structure to beneficial and detrimental actions. *Annu. Rev. Pharmacol. Toxicol.* 21:265–293.

Kuo, S.-M., and P.S. Aronson. 1988. Oxalate transport via the sulfate/HCO_3 exchanger in rabbit renal basolateral membrane vesicles. *J. Biol. Chem.* 263:9710–9717.

Kurtz, I., G. Nagami, N. Yanagawa, L. Li, C. Emmons, and I. Lee. 1994. Mechanism of apical and basolateral Na^+-independent Cl^-/base exchange in the rabbit superficial proximal straight tubule. *J. Clin. Invest.* 94:173–183.

Lee, B.S., R.B. Gunn, and R.R. Kopito. 1991. Functional differences among nonerythroid anion exchangers expressed in a transfected human cell line. *J. Biol. Chem.* 266:11448–11454.

Marletta, M.A., P.S. Yoon, R. Iyengar, C.D. Leaf, and J.S. Wishnok. 1988. Macrophage oxidation of l-arginine to nitrite and nitrate: nitric oxide is an intermediate. *Biochemistry.* 27:8706–8711.

Mehrag, A.A., and M.R. Blatt. 1995. NO_3^- transport across the plasma membrane of *Arabidopsis thaliana* root hairs: kinetic control by pH and membrane voltage. *J. Membr. Biol.* 145:49–66.

Melnik, E., R. Latorre, J.E. Hall, and D.C. Tosteson. 1977. Phloretin-induced changes in ion transport across lipid bilayer membranes. *J. Gen. Physiol.* 69:243–257.

Milstien, S., N. Sakai, B.J. Brew, C. Krieger, J.H. Vickers, K. Saito, and M.P. Heyes. 1994. Cerebrospinal fluid nitrite/nitrate levels in neurologic diseases. *J. Neurochem.* 63:1178–1180.

Miwa, M., D.J. Stuehr, M.A. Marletta, J.S. Wishnok, and S.R. Tannenbaum. 1987. N-nitrosamine formation by macrophages. *IARC Scientific Publications.* 84:340–344.

Miwa, M., M. Watanabe, T. Nishida, and K. Shinohara. 1991. Macrophages produce nitrite, nitrate and nitrosamines after addition of catalase. *IARC Scientific Publications.* 105:388–391.

Munzel, T., H. Sayegh, B.A. Freeman, M.M. Tarpey, and D.G. Harrison. 1995. Evidence for enhanced vascular superoxide anion production in nitrate tolerance. *J. Clin. Invest.* 95:187–194.

Ohshima, H., T.Y. Bandaletova, I. Brouet, H. Bartsch, G. Kirby, F. Ogunbiyi, V. Vatanasapt, and V. Pipitgool. 1994. Increased nitrosamine and nitrate biosynthesis mediated by nitric oxide synthase induced in hamsters infected with liver fluke (opisthorchis viverrini). *Carcinogenesis.* 15:271–275.

Oudenhoven, I.M., H.L. Klaasen, J.A. Lapre, A.H. Weerkamp, and R. van d. Meer. 1994. Nitric oxide-derived urinary nitrate as a marker of intestinal bacterial translocation in rats. *Gastroenterology.* 107:47–53.

Palfrey, H.C., and S. Leung. 1993. Inhibition of Na-K-2Cl cotransport and bumetanide binding by ethacrynic acid, its analogues, and adducts. *Am. J. Physiol.* 264:C1270–C1277.

Parker, J.C. 1983. Hemolytic action of potassium salts on dog red blood cells. *Am. J. Physiol.* 244:C313–C317.

Parker, J.C., and V. Castranova. 1984. Volume-responsive sodium and proton movements in dog red blood cells. *J. Gen. Physiol.* 84: 379–401.

Poole, R.C., and A.P. Halestrap. 1993. Transport of lactate and other monocarboxylates across mammalian plasma membranes. *Am. J. Physiol.* 264:C761–C782.

Reinertsen, K.V., T.I. Tonnessen, J. Jacobsen, K. Sandvig, and S. Olsnes. 1989. Role of chloride/bicarbonate antiport in the control of cytosolic pH. *J. Biol. Chem.* 263:11117–11125.

Rentsch, D., M. Laloi, I. Rouhara, E. Schmelzer, S. Delrot, and W.B. Frommer. 1995. NTR1 encodes a high affinity oligopeptide transporter in *Arabidopsis. FEBS Letts.* 370:264–268.

Roos, A., and W.F. Boron. 1981. Intracellular pH. *Physiol. Rev.* 61: 296–434.

Rotin, D., and S. Grinstein. 1989. Impaired cell volume regulation in Na^+/H^+ exchange deficient mutants. *Am. J. Physiol.* 267: C1158–C1165.

Schmidt, H.H.H., R. Seifert, and E. Bohme. 1989. Formation and release of nitric oxide from human neutrophils and HL-60 cells induced by a chemotactic peptide, platelet activating factor and leukotriene B_4. *FEBS Letts.* 244:357–360.

Schron, C.M., R.G. Knickelbein, P.S. Aronson, J. Della Puca, and J.W. Dobbins. 1985. Effects of cations on pH gradient-stimulated sulfate transport in rabbit ileal brush-border membrane vesicles. *Am. J. Physiol.* 249:G614–G621.

Schron, C.M., R.G. Knickelbein, P.S. Aronson, and J.W. Dobbins. 1987. Evidence for carrier-mediated Cl-SO_4 exchange in rabbit ileal basolateral membrane vesicles. *Am. J. Physiol.* 253:G404–G410.

Sever, R., T. Cook, and V. Cattell. 1992. Urinary excretion of nitrite and nitrate in experimental glomerulonephritis reflects systemic immune activation and not glomerular synthesis. *Clin. Exp. Immunol.* 90:326–329.

Sheu, J.N., R. Quigley, and M. Baum. 1995. Heterogeneity of chloride/base exchange in rabbit superficial and juxtamedullary proximal convoluted tubules. *Am. J. Physiol.* 268:F847–F853.

Shi, Y., H.Q. Li, C.K. Shen, J.H. Wang, S.W. Qin, R. Liu, and J. Pan. 1993. Plasma nitric oxide levels in newborn infants with sepsis. *J. Pediatr.* 123:435–438.

Shrode, L.D., J.D. Klein, W.C. O'Neill, and R.W. Putnam. 1995. Shrinkage-induced activation of the Na^+/H^+ exchange in primary rat astrocytes: role of myosin light chain kinase. *Am. J. Physiol.* 269:C257–C266.

Simchowitz, L. 1988. Interactions of bromide, iodide, and fluoride with the pathways of chloride transport and diffusion in human neutrophils. *J. Gen. Physiol.* 91:835–860.

Simchowitz, L., and A.O. Davis. 1989. Sulfate transport in human neutrophils. *J. Gen. Physiol.* 94:95–124.

Stuehr, D.J., and M.A. Marletta. 1987*a*. Induction of nitrite/nitrate synthesis in murine macrophages by BCG infection, lymphokines, or interferon-gamma. *J. Immunol.* 139:518–525.

Stuehr, D.J., and M.A. Marletta. 1987*b*. Further studies on murine macrophage synthesis of nitrite and nitrate. *Iarc Scientific Publications.* 84:335–339.

Stuehr, D.J., and M.A. Marletta. 1987*c*. Synthesis of nitrite and nitrate in murine macrophage cell lines. *Cancer Res.* 47:5590–5594.

Swallow, C.J., S. Grinstein, R.A. Sudsbury, and O.D. Rotstein. 1991. Nitric oxide derived from l-arginine impairs cytoplasmic pH regulation by vacuolar-type H^+ ATPases in peritoneal macrophages. *J. Exp. Med.* 174:1009–1021.

Tanaka, S., W. Kamiike, T. Ito, F. Uchikoshi, H. Matsuda, M. Nozawa, E. Kumura, T. Shiga, and H. Kosaka. 1995. Generation of nitric oxide as a rejection marker in rat pancreas transplantation. *Transplantation.* 60:713–717.

Thomas, J.A., R.N. Buchsbaum, A. Zimniak, and E. Racker. 1979. Intracellular pH measurements in Ehrlich ascites tumour cells utilizing spectroscopic probes generated in situ. *Biochemistry.* 18:2210–2218.

Tsay, Y.-F., J.I. Schroeder, K.A. Feldmann, and N.M. Crawford. 1993. The herbicide sensitivity gene *CHL1* of Arabidopsis encodes a nitrate-inducible nitrate transporter. *Cell.* 72:705–713.

Verdon, C.P., B.A. Burton, and R.L. Prior. 1995. Sample pretreatment with nitrate reductase and glucose-6- phosphate dehydrogenase quantitatively reduces nitrate while avoiding interference by $NADP^+$ when the Griess reaction is used to assay for nitrite. *Anal. Biochem.* 224:502–508.

Veszelovszky, E., N.H.G. Holford, L.L. Thomsen, R.G. Knowles, and B.C. Baguley. 1995. Plasma nitrate clearance in mice: modeling of the systemic production of nitrate following the induction of nitric oxide synthesis. *Cancer Chemother. Pharmacol.* 36:155–159.

Wang, X., R.C. Poole, A.P. Halestrap, and A.J. Levi. 1993. Characterization of the inhibition by stilbene disulphonates and phloretin of lactate and pyruvate transport into rat and guinea-pig cardiac myocytes suggests the presence of two kinetically distinct carriers in heart cells. *Biochem. J.* 290:249–258.

Weinberg, J.B., M.A. Misukonis, P.J. Shami, S.N. Mason, D.L. Sauls, W.A. Dittman, E.R. Wood, G.K. Smith, B. McDonald, K.E. Bachus, et al. 1995. Human mononuclear phagocyte inducible nitric oxide synthase (iNOS): analysis of iNOS mRNA, iNOS protein, biopterin, and nitric oxide production by blood monocytes and peritoneal macrophages. *Blood.* 86:1184–1195.

Weiss, G., H. Schwaighofer, M. Herold, D. Nachbaur, H. Wachter, D. Niederwieser, and E.R. Werner. 1995. Nitric oxide formation as predictive parameter for acute graft-versus-host disease after human allogeneic bone marrow transplantation. *Transplantation.* 60:1239–1244.

Winlaw, D.S., C.G. Schyvens, G.A. Smythe, Z. Du, S.P. Rainer, A.M. Keogh, J.A. Mundy, R.S. Lord, P.M. Spratt, and P.S. MacDonald. 1994. Urinary nitrate excretion is a noninvasive indicator of acute cardiac allograft rejection and nitric oxide production in the rat. *Transplantation.* 58:1031–1036.

Wright, C.D., A. Mulsch, R. Busse, and H. Osswald. 1989. Generation of nitric oxide by human neutrophils. *Biochem. Biophys. Res. Commun.* 160:813–819.

Wright, C.E., D.D. Rees, and S. Moncada. 1992. Protective and

pathological roles of nitric oxide in endotoxin shock. *Cardiovasc. Res.* 26:48–57.

Zhang, J., Y. Feng, and M. Forgac. 1994. Proton conduction and bafilomycin binding by the V_o domain of the coated vesicle V-ATPase. *J. Biol. Chem.* 269:23518–23523.

Zhang, Z.-H., and A.K. Solomon. 1992. Effect of pCMBS on anion transport in human red cell membranes. *Biochim. Biophys. Acta.* 1106:31–39.

Zhao, H., X. Xu, K. Ujiie, R.A. Star, and S. Muallem. 1994. Transport and interaction of nitrogen oxides and NO_2 with CO_2^- HCO_3^- transporters in pancreatic acini. *Am. J. Physiol.* 267:C385–C393.